Biol. Cybern. 78, 319–327 (1998)

Biological Cybernetics

Standing sway: iterative estimation of the kinematics and dynamics of the lower extremities from force-plate measurements

O. Levin[1], J. Mizrahi[1], M. Shoham[2]

[1] Department of Biomedical Engineering, Technion – Israel Institute of Technology, Haifa 32000, Israel
[2] Department of Mechanical Engineering, Technion – Israel Institute of Technology, Haifa 32000, Israel

Received: 22 July 1997 / Accepted in revised form: 29 January 1998

Abstract In this study, a model for the estimation of the dynamics of the lower extremities in standing sway from force plate data only is presented. A three-dimensional, five-segment, four-joint model of the human body was used to describe postural standing sway dynamics. Force-plate data of the reactive forces and centers of pressure were measured bilaterally. By applying the equations of motion to these data, the transversal trajectory of the center of gravity (CG) of the body was resolved in the sagittal and coronal planes. An inverse kinematics algorithm was used to evaluate the kinematics of the body segments. The dynamics of the segments was then resolved by using the Newton-Euler equations, and the model's estimated dynamic quantities of the distal segments were compared with those actually measured. Differences between model and measured dynamics were calculated and minimized, using an iterative algorithm to re-estimate joint positioning and anthropometric properties. The above method was tested with a group of 11 able-bodied subjects, and the results indicated that the relative errors obtained in the final iteration were of the same order of magnitude as those reported for closed loop problems involved in direct kinematics measurements of human gait.

1 Introduction

Knowledge of the kinematics and dynamics of the lower extremities in human gait and postural sway is essential for gaining quantitative information on the muscle forces, mechanical impedance and power transfer through the joints. In previous studies the internal forces and torques in the joints were resolved on the basis of direct measurements of the kinematics of the body segments and of the foot-ground reactions (Fioretti et al. 1992a,b; Penzer et al. 1995; Vaughan et al. 1982a,b). Whole-body kinematics was also measured in clinical practice in an attempt to understand the role of the motor feedback elements (i.e., visual, vestibular, and proprioceptive) in stabilizing the body (Andersson and Winters 1990; Barin 1989; Keshner and Allum 1990; Penzer et al. 1995; Snijders and Verduin 1973; Valk-Fai 1973). Three-dimensional measurements of the kinematics of the body require at least two cameras and an array of markers. For the measurements of sway motion during standing, in which the peak-to-peak sway amplitudes of the body's center of gravity (CG) were reported to be less than 10 mm, the resolution is limited to ± 1 mm for position and ± 1 deg for orientation (Benda et al. 1994; Riley et al. 1990).

In a previous study (Levin and Mizrahi 1996), we presented a method for the evaluation of the trajectory of the CG and the kinematics of the segments from bilateral force-plate measurements only, i.e., without measurement of body kinematics. When using two force platforms, the force components and centers of pressure on each foot can be measured separately. This is essential if standing sway is to be modeled in terms of multisegment dynamics (Levin and Mizrahi 1996), which accounts for possible asymmetries.

It should be mentioned, however, that irrespective of the method used, the procedures for acquiring the kinematics and dynamics of the body segments involve two sources of uncertainty: (a) joint positioning with respect to the point of application of the reaction forces (Vaughan et al. 1982b) and to the location of the markers and (b) anthropometry of the subject and his segments.

In this study, we develop a model for the estimation of the dynamics of the lower extremities in standing sway from force-plate data only. The errors in evaluation of the model dynamics were minimized by the application of an iterative optimization procedure. In each iteration, positioning of the joints and the subject's anthropometry were readjusted to minimize the differences between the model and measured dynamic data.

Correspondence to: J. Mizrahi (Fax: +972-4-823-4131)

2 Model

2.1 Kinematics

A three-dimensional, four-joint, five-segment model of the human body was used to describe postural sway dynamics during standing still, as described in Fig. 1. The two lower segments of each leg, representing the feet, were assumed to be attached to the supporting platforms and, therefore, to form together one link. The model was thus identified as a spatial four-bar mechanism interconnected by four joints, each allowing rotation about two axes. Although the hip is known to resemble a ball and socket joint, we assumed that the rotation of the HAT (head, arms, and trunk) segment of the model about its vertical (z) axis was negligible. From an analysis of mobility (Hunt 1978), it can be shown that the model in Fig. 1 has two independent degrees of freedom. For the right ankle joint (no. 1), we assigned the generalized coordinates ψ_1 and θ_1 as the free independent coordinates of the model in the sagittal and coronal planes, respectively. For joints 2 (right hip), 3 (left hip), and 4 (left ankle) the respective ψ_i and θ_i coordinates were described as linear combinations of ψ_1 and θ_1, assuming small motions. The coordinate axes were defined as follows: x and y along the dimensional axes of each forceplate, and z perpendicular to the plane of the forceplate (Fig. 1). It has been reported that such a model is adequate to represent the nearly horizontal motion of the CG in standing sway of healthy and pathological subjects (Kapteyn 1973; Saunders et al. 1953; Snijders and Verduin 1973).

Figure 1 also shows the external forces applied on a subject standing on a pair of force platforms. The vectors $\mathbf{r}_{\mathrm{pR}}$ and $\mathbf{r}_{\mathrm{pL}}$ denote, respectively, the points of application of the resultant reactive forces $\mathbf{F}_{\mathrm{R}}$ and $\mathbf{F}_{\mathrm{L}}$ about the right (O_{R}) and left (O_{L}) centers of the platforms. The moments of the forces $\mathbf{F}_{\mathrm{R}}$ and $\mathbf{F}_{\mathrm{L}}$ about O_{R} and O_{L} are denoted by $\mathbf{M}_{\mathrm{R}}$ and $\mathbf{M}_{\mathrm{L}}$, respectively. The position vectors to the CG of the body from the platform centers O_{R} and O_{L} are denoted by $\mathbf{r}_{\mathrm{GR}}$ (shown in Fig. 1) and $\mathbf{r}_{\mathrm{GL}}$, respectively. The following moment equation of motion can be written:

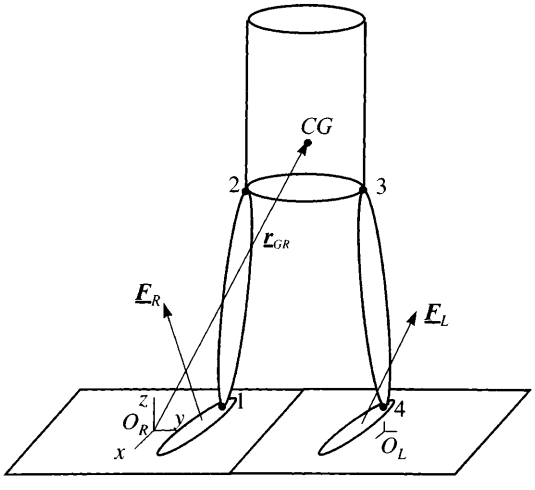

Fig. 1. Five-segment model of the swaying human body, in standing still posture. The reaction force $\mathbf{F}_R$ and $\mathbf{F}_L$ are measured bilaterally from both feet. The position vectors to the Center of gravity (CG) from the center O_R is denoted by $\mathbf{r}_{GR}$

$$\mathbf{M}_{\mathrm{R}} + \mathbf{M}_{\mathrm{L}} - (\mathbf{r}_{\mathrm{GR}} \times \mathbf{F}_{\mathrm{R}}) - (\mathbf{r}_{\mathrm{GL}} \times \mathbf{F}_{\mathrm{L}}) = \dot{\mathbf{H}} \tag{1}$$

where $\dot{\mathbf{H}}$ represents the time rate change of the angular momentum about the body's CG. This term was shown to be negligible in postural sway during standing still (Levin and Mizrahi 1996). It is also assumed that the movement of the body's CG takes place in the transverse plane, with a constant distance from the ground, $r_{\mathrm{GR}z}$. This distance was assumed to be 55% of the subject's total height, above the platform's plane (Saunders et al. 1953). Thus, with $\dot{\mathbf{H}} \cong 0$, we can express from (1) the approximate transverse components of the CG ($r_{\mathrm{GR}x}$, $r_{\mathrm{GR}y}$) as follows:

$$r_{\mathrm{GR}x} = -\frac{M_{\mathrm{R}y} + M_{\mathrm{L}y}}{F_{\mathrm{R}z} + F_{\mathrm{L}z}} + r_{\mathrm{GR}z}\frac{F_{\mathrm{R}x} + F_{\mathrm{L}x}}{F_{\mathrm{R}z} + F_{\mathrm{L}z}} + r_{\mathrm{RL}x}\frac{F_{\mathrm{L}z}}{F_{\mathrm{R}z} + F_{\mathrm{L}z}} \tag{2a}$$

$$r_{\mathrm{GRy}} = \frac{M_{\mathrm{R}x} + M_{\mathrm{L}x}}{F_{\mathrm{R}z} + F_{\mathrm{L}z}} + r_{\mathrm{GR}z}\frac{F_{\mathrm{R}y} + F_{\mathrm{L}y}}{F_{\mathrm{R}z} + F_{\mathrm{L}z}} + r_{\mathrm{RL}y}\frac{F_{\mathrm{L}z}}{F_{\mathrm{R}z} + F_{\mathrm{L}z}} \tag{2b}$$

The vector connecting the centers of the platforms $\mathbf{r}_{\mathrm{RL}}$ ($r_{\mathrm{RL}x}$, $r_{\mathrm{RL}y}$, $\mathrm{r}_{\mathrm{RL}z}$) can be written as:

$$\mathbf{r}_{\mathrm{RL}} = \mathbf{r}_{\mathrm{GR}} - \mathbf{r}_{\mathrm{GL}} \tag{3}$$

It is noted from Fig. 1 that the platforms lie in the same plane and their y-axes are collinear; hence, $r_{\mathrm{RL}x} = r_{\mathrm{RL}z} = 0$.

The position of the CG is denoted by the vector $\mathbf{r}_{\mathrm{GR}}(r_{\mathrm{GR}x}, r_{\mathrm{GR}y}, r_{\mathrm{GR}z})$, with respect to the inertial coordinate system $\hat{e}_0$, located at the origin O_{R} (center of the right platform). The following local coordinate systems were located at the centers of the joints used: $\hat{e}_1$ for the right leg, $\hat{e}_2$ for HAT, $\hat{e}_4$ for the left leg, and $\hat{e}_3$ located in the left hip, which served as the end-point for each of the two kinematic chains: 1-2-3 and 1-4-3 (Fig. 1). Thus, the location of the CG with respect to $\hat{e}_1$ is denoted by $\mathbf{r}_{\mathrm{G}}(r_{\mathrm{G}x}, r_{\mathrm{G}y}, r_{\mathrm{G}z})$. The time-dependent components of the CG, with respect to the $\hat{e}_1$ coordinate system, are expressed by the following vector equation:

$$\mathbf{r}_{\mathrm{G}} = [\mathbf{A}_{\theta 1}][\mathbf{A}_{\psi 1}]\ (\mathbf{l}_{12} + [\mathbf{A}_{\theta 2}][\mathbf{A}_{\psi 2}]\mathbf{l}_{2\mathrm{CG}}) \tag{4}$$

and, more generally, $[\mathbf{A}_{\theta i}]$ and $[\mathbf{A}_{\psi i}]$ are rotation matrices of θ_i and ψ_i, respectively, about the local coordinate system $\hat{e}_i$ ($i = 1 \ldots 4$).

The vector from the right ankle (point 1) to the right hip (point 2) is denoted by $\mathbf{l}_{12}$, and the vector from the right hip to the CG of the body is denoted by $\mathbf{l}_{2\mathrm{CG}}$. The following kinematic constraints result:

$$[\mathbf{A}_{\theta 1}][\mathbf{A}_{\psi 1}](\mathbf{l}_{12} + [\mathbf{A}_{\theta 2}][\mathbf{A}_{\psi 2}]\mathbf{l}_{23}) - (\mathbf{r}_{14} + [\mathbf{A}_{\theta 4}][\mathbf{A}_{\psi 4}]\mathbf{l}_{34}) = 0 \tag{5}$$

$\mathbf{l}_{23}$ is the vector from right hip (joint 2) to left hip (joint 3), and $\mathbf{l}_{43}$ from the left ankle (joint 4) to the left hip

(joint 3). The vector from the right ankle to the left ankle is denoted by $\mathbf{l}_{14}$. The anthropometric dimensions in (4) and (5), i.e., the components of the position vectors $\mathbf{l}_{12}$ $\mathbf{l}_{23}$ $\mathbf{l}_{34}$ and $\mathbf{l}_{2CG}$, were evaluated in their respective local systems by scaling data taken from the literature (Braune and Fischer 1987; Drillis and Contini 1966). The lateral components of the position vector $\mathbf{l}_{14}$ were determined from the foot positioning of the subjects. The vertical component of $\mathbf{l}_{14}$, giving the difference between the heights of the right and the left ankles with respect to the plane of the platform, was assumed to be zero. It should be noted that in (4), the components of the spatial location of the CG, expressed in the inertial system as r_{Gx}, r_{Gy} and r_{Gz} refer to the right ankle (joint 1, Fig. 1). Since the components of the approximate spatial location of CG are given for the center of the right platform, the following transformation is required:

$$\begin{aligned} r_{Gx}(t) - r_{GRx}(t) &= r_{ox} \\ r_{Gy}(t) - r_{GRy}(t) &= r_{oy} \\ r_{Gz}(t) - r_{GRz}(t) &= r_{oz} \end{aligned} \tag{6}$$

where r_{ox} and r_{oy} are the lateral components of the vector $\mathbf{r}_o$ from the center of the right platform (O_R) to the center of the right ankle. The term r_{oz} is the vertical distance from the center of the right ankle to the platform plane.

By combining (4) and (5), a system of six nonlinear equations is generated:

$$\mathbf{f}(\theta, \psi, \mathbf{r}_G, \mathbf{l}) = 0 \tag{7}$$

where

$$\theta = [\theta_1(t), \theta_2(t), \theta_3(t), \theta_4(t)] \text{ and}$$
$$\psi = [\psi_1(t), \psi_2(t), \psi_3(t), \psi_4(t)]$$

and $\mathbf{l}$ represents the set of anthropometric properties including the components of the position vectors $\mathbf{l}_{12}$, $\mathbf{l}_{23}$, $\mathbf{l}_{34}$ $\mathbf{l}_{2CG}$ and $\mathbf{l}_{14}$.

The nonlinear set of (7) was solved with the Newton-Raphson method. Selection of the starting vector used to initiate the computation was based on the results obtained in our previous study (Levin and Mizrahi 1996), showing that the posture of able-bodied subjects was found to be close to symmetry, with respect to the sagittal plane of the body. Thus, the coordinates of the starting vector were evaluated to comply with symmetrical positioning of the segments with respect to the sagittal plane of the model. It should be noted though that the asymmetry due to the medio-lateral shift of the average position of the CG for subjects with pathologies was found to be five- to seven-fold larger [$P < 0.005$, Levin and Mizrahi (1996)] than that of able-bodied subjects. The CG location was found to be shifted towards the sound leg. In this case, the average medio-lateral position of the CG is to be taken into account whilst evaluating the components of the starting vector. By solving (7), we evaluated the instantaneous displacements of the generalized coordinates as a function of a given instantaneous displacement of the CG.

2.2 Dynamics

The Newton-Euler equations were used to convert the generalized coordinates ψ and θ into the angular and linear velocities and acceleration vectors of the segments (Fig. 2). Forces and moments in the joints were calculated backwards by using the Newton-Euler equations of motion. The vector from the left ankle to the point of application of $\mathbf{F}_L$ is denoted by $\mathbf{r}_{4p}$. The internal force and moment acting on the left ankle (point 4) can be calculated as follows:

$$\mathbf{F}_4 = \mathbf{F}_L + m_{fL} \cdot \mathbf{g} \tag{8}$$
$$\mathbf{M}_4 = \mathbf{r}_{4p} \times \mathbf{F}_L \tag{9}$$

where m_{fL} is the mass of the left foot, and $\mathbf{g}$ is the acceleration due to gravity, acting on the center of mass (**CM**) of the left foot. The model-predicted foot-ground reaction force acting on the right foot is denoted by $\mathbf{R}_R$ and was estimated as follows:

$$\mathbf{R}_R = -(\mathbf{F}_1 + m_{fR} \cdot \mathbf{g}z) \tag{10}$$

where $\mathbf{F}_1$ is the estimated force on the right ankle (joint 1) and m_{fR} denotes the mass of the right foot.

The model presented here is confirmed by comparing the components of the estimated reaction $\mathbf{R}_R$ (Eq. 10) with the actually measured $\mathbf{F}_R$ reaction at the right foot and, similarly, by comparing the estimated and calculated components of the moment about the right ankle $\mathbf{M}_1$:

$$\mathbf{M}_1 = \mathbf{r}_{1p} \times \mathbf{F}_R \tag{11}$$

where $\mathbf{r}_{1p}$ is the vector connecting the right ankle to the point of application of $\mathbf{F}_R$. However, differences between measured and model results may also arise, within certain limits, due to the following reasons: (a) error in estimating the ankle positioning with respect to the platform origins; (b) error in estimating the anthropometric properties of the segments; (c) drift in the static values of the measured forces, due to the nature of the piezoelectric transducers. Quantitative evaluation of the difference between the model and the measured components of the forces and the moments was obtained by using the mean square difference:

$$E = \frac{1}{n}\sum_{i=1}^{n} [q_{est}(i) - q_{meas}(i)]^2 \tag{12}$$

where $q_{est}(i)$ is the model value at time point i, $q_{meas}(i)$ is the measured value at time point i, and n is the number of data points in the time history record.

An iterative algorithm (Fig. 2) was developed to minimize the average error E. The iteration process allowed for the readjustment of the positioning of the center of the ankles and hips. In the first iteration, this positioning was set as the intersection between the approximated midline and the talocrural axes of the foot. In the iterative process, the following constraints were imposed.

(a) The distance between the re-estimated location of the ankle, obtained for the ith iteration, and inter-

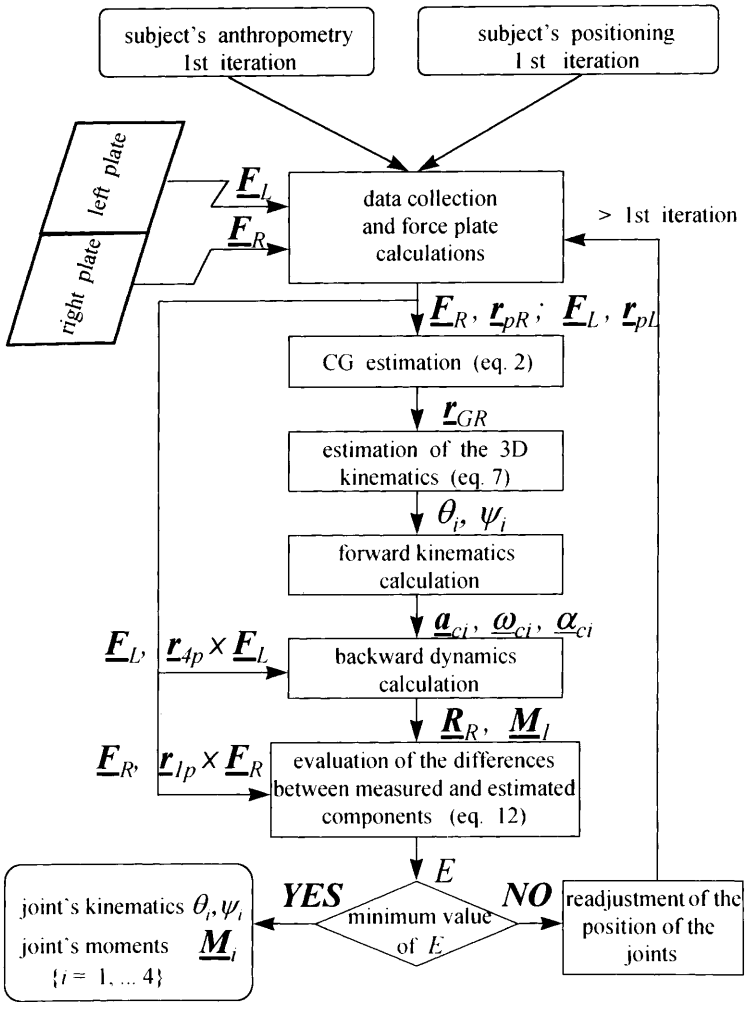

Fig. 2. Block diagram of the model. Kinematics of the segments were estimated directly from the trajectory of the CG, which was evaluated from force-plate measurements. Forces and moments acting on the model's distal segments were then resolved by means of backwards dynamics calculations. Differences between model ($\mathbf{R}_R$ and $\mathbf{M}_I$) and measured ($\mathbf{F}_R$ and $\mathbf{r}_{1p} \times \mathbf{F}_R$) dynamics of the right foot were minimized by readjustment of the positioning of the joints and the anthropometric properties of the segments. Kinematics (θ_i, ψ_i) and dynamics ($\boldsymbol{M}_i$) of the segments were estimated afterwards

cept point between the talocrural and midline foot axes should not exceed the predetermined upper limit of 0.12 l_{foot} along the midline axis of the foot and of 0.08 l_{foot} along the talocrural axis. Within these values, the tibia talus and calcaneus were found to overlap (Inman 1976) (l_{foot} determines the distance from the tip of the big toe to the posterior edge of the calcaneus).

(b) The estimated trajectory of the centers of pressure, denoted by $\mathbf{r}_{1\text{p}}$ (right foot) and $\mathbf{r}_{4\text{p}}$ (left foot) should remain within the boundaries of the foot (known for each subject).

(c) The mediolateral distance between the hips should not exceed 10% of its initial value, which was evaluated by using given anthropometric data (Drillis and Contini 1966). The other anthropometric parameters including the components of $\mathbf{l}_{12}$, $\mathbf{l}_{23}$ and $\mathbf{l}_{2\text{CG}}$ were assumed to remain constant during the iterative process.

2.3 Range of applicability of the model

The range of applicability of the model is imposed by the requirement of convergence of the above-described iterative process. The model limitations originate from two sources: (i) error in positioning of the feet on the force platforms and (ii) requirements of keeping the feet flat on the platforms.

(i) The difference between actual and preset positioning of the feet on the platforms should be limited. This requirement follows if the constraints listed in the above-described iterative algorithm, related to location of the ankles and distance between the hips, are to be fulfilled. Expressed in terms of the intercept point between the talocrural and midline foot axes, the following limitation is obtained:

$$\left[\Delta x_{\text{R,L}}^2 + \Delta y_{\text{R,L}}^2\right]^{1/2} \leq 0.14\,\ell_{\text{foot}} \tag{13}$$

where $\Delta x_{\text{R,L}}$ and $\Delta y_{\text{R,L}}$ are the positioning errors along the x and y axes (Fig. 1) of the right or left feet.

(ii) Although the formulation of the above model is suited for subjects while standing still, the methodology can be extended to any body motion that can be performed while keeping the feet flat on the platform surface, such as actively swaying the body or doing a sudden hip flexor motion. It may be noted, though, that in cases where the resulting sway

becomes considerably increased, the time rate change of the angular momentum about the body is CG, $\dot{\mathbf{H}}$ [right hand side of (1)] may not be negligible anymore. In this case, the model would have to be reformulated, taking into account the term $\dot{\mathbf{H}}$. Another significant change in the extended model may refer to the necessity of estimation of the vertical displacements of the CG, which in the present study was assumed to be zero.

3 Experimental methods

3.1 Apparatus and data collection

The foot-ground reaction forces from both feet were measured by two Kistler force platforms (type Z-4304). The signals collected from the platforms, sampled at 100 samples per s, enabled us to calculate the application point of the measured forces, due to the known geometric location of the piezoelectric transducers. Every test lasted 30 s, of which the middle 20 s were sampled, and the collected data included: forces, points of application, and moments. The testing procedure was reviewed by the local ethics committee and was performed in accordance with the ethical standards of the Declaration of Helsinki.

Prior to the tests on subjects, a calibration procedure of the coordinates of the points of application of force on the platforms was performed as follows. A vertical load of 200 N was applied on each platform through a Teflon plunger with a contact diameter of 2 mm. The point of application of the load was varied by intervals of 5 mm along and across a rectangular grid whose axes were parallel to those of the platforms. These calibration intervals were enforced in the measuring area of the platforms, i.e., their two medial halves: the right half of the left platform and the left half of the right platform. Outside the measuring area, the calibration intervals were set to 10 mm. The calibration obtained served to correct the actual output coordinates in accordance with the expected coordinates. Additionally, the short-term drift of the platforms was tested and found negligible: for a measuring period of 30 s, the drift was less than 1 mm in the coordinate outputs. The zero shift of the forces and centers of pressure due to long-term drift was corrected by setting to zero the average value obtained from summing, over the sampling time, each of the **CG** acceleration (sum of all external forces) and external moments.

3.2 Subjects and protocol

Eleven subjects took part in this study. All subjects gave their informed consent prior to their inclusion. The subjects were able-bodied, with no known history of injury or pathological disorders which could affect normal posture or gait. Their average age was 41.3 ± 7.5 years (range 28–49 years); their average height was 173.7 ± 9.5 cm (range 155–188 cm); and their average mass was 77.4 ± 12.3 kg range 62–99 kg). All subjects were asked to stand still with their eyes closed, barefoot, on the platforms, one leg on each platform. The positioning of the feet was similar for all subjects and was symmetrical in relation to the line separating the platforms. Spacing between the subject's feet was set to 30 cm. Every test was repeated four times for each subject.

3.3 Iterative algorithm

The measured foot-ground reactive forces and centers of pressure were entered in the algorithm presented in Fig. 2. In the first iteration, the initial position of the center of the ankles was set in accordance with the approximate positioning of the foot (at $x_1 = x_4 = -5\,\text{cm}$; $y_1 = 15\,\text{cm}$; $y_4 = 45\,\text{cm}$ in relation to the coordinate system $\hat{e}_0$). In the subsequent iterations, the mean square differences between model and measured dynamics were evaluated (12), and minimized by readjusting the position of the joints. The iterative process was stopped when either of the following occurred: (a) the minima of the mean square difference of each of the dynamic terms was reached, or (b) the minima was not reached after a certain number of iterations (as imposed by the MATLAB routine) was exceeded.

In the present study, 15 of the 44 tests were excluded because of convergence difficulties. The average peak-to-peak excursion of the center of pressure in the anteroposterior direction was 1.00 cm for the converging tests and 2.03 cm for the non-converging tests. These values shed light on the sway limits within which the described algorithm converges. Two of the remaining 29 tests were discarded due to an excessive mean square difference value (E), which resulted in comparing the intra- and intersubject average. The mediolateral force and the torque in the coronal plane were 2.73 N and 3.77 Nm in one subject and 7.33 N and 11.4 Nm in the other, as compared with average values (for the remaining 27 tests) of 0.37 ± 0.18 N and 0.87 ± 0.49 Nm. The results presented will, therefore, include a total of 27 tests for the 11 subjects.

4 Results

Typical model and measured (force plate) patterns of the components of the ground reaction force are presented in Fig. 3 (subject El). The forces are almost identical for the measured (solid line) and estimated (dotted line) components of the vertical and mediolateral directions. On the other hand, the anteroposterior components differed more, but with the patterns still remaining sequential. The data measured by the right force plate (force and center of pressure) served to establish 'measured' torques in the coronal (M_{1x}) and sagittal (M_{1y}) planes (11), acting on the right ankle (dotted line). These components are given in Fig. 4, together with the

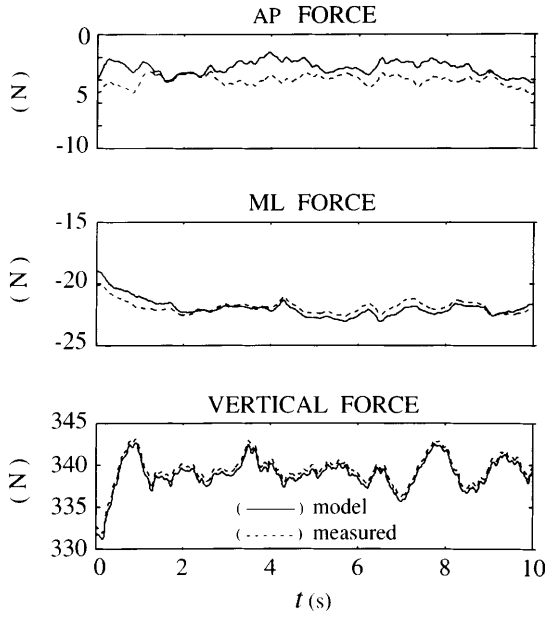

Fig. 3. Model ($\mathbf{R}_R$ *solid line*) and measured ($\mathbf{F}_R$ *dotted line*) components of the reaction forces acting on the right foot (AP = anteroposterior direction, ML = mediolateral direction)

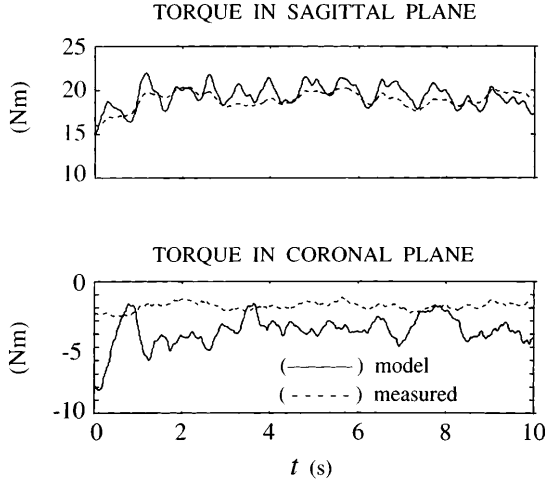

Fig. 4. Model ($\mathbf{M}_1$ *solid curve*) and measured ($\mathbf{r}_{1p} \times \mathbf{F}_R$) components of the moments acting on the right foot

torques estimated by the model (solid line). There is a considerable difference between the amplitude of the model estimated (solid line) and the measured (dotted line) components of the torque in the coronal plane. A relatively good agreement was obtained in the sagittal plane, both in amplitude and sequence between the model and measured components.

To provide the basis for quantitative evaluation of the difference between the estimated (model, Fig. 2) and the measured (force plate)/calculated (11) components of the torques and forces, the following error function, suggested by Vaughan et al. (1982b), was used:

$$\varepsilon = \frac{1}{T}\int_{o}^{T} |q(t) - \hat{q}(t)|\, \mathrm{d}t \tag{14}$$

where $q(t)$ is the measured experimentally obtained component and $\hat{q}(t)$ is the estimated component. T is the sampling period for which the error is integrated. Table 1 presents the value of the average ± SD over $n = 27$ trials obtained by the data collected from $n = 11$ able-bodied subjects. The error (14) was divided by the root mean square (RMS) measured values of the force or torque in order to gain a quantitative relative (%) error. The average relative errors were: 0.34% ± 0.25% for the vertical forces, 1.97% ± 1.12% for the mediolateral forces, and 15.7% ± 14.8% for the torques in the sagittal plane. Relatively large errors were found for the anteroposterior forces, 62.7% ± 64.2%, and the torque in the coronal plane, 33.4% ± 43.8%.

The patterns of the angular displacements in the sagittal and coronal planes are given in Fig. 5. Interestingly, the generalized coordinates in the coronal or the sagittal plane were in sequence (in phase or in opposite phase). The relation between these coordinates shows that the angular displacements in the left and right ankles are in phase, both in the coronal (θ_1 and θ_4) and sagittal (ψ_1 and ψ_4) planes. The angular displacements in the right ankle were found to be in opposite phase with the right hip, both in the coronal (θ_1 and θ_2) and sagittal (ψ_1 and ψ_2) planes. Similar angular displacements were found on the left side (i.e., θ_4 and ψ_4 are in opposite phase with θ_3 and ψ_3, respectively).

Comparison of the estimated kinematic results with measurements reported in the literature is presented in Table 2. Attention should be paid to differences existing in the methodologies and tested populations between the compared studies. It was thus concluded that ranges of motion, rather than means, are more appropriate for comparison. Nevertheless, the data of Fioretti et al. (1992b) were represented in terms of mean and standard deviation, since the ranges were not available in their study. The ranges of the two other studies (Valk-Fai 1973; Corradini et al. 1997) compared well with our model results.

Table 1. Error estimates for the predicted components of force and torque at the right foot [mean (SD) of all subjects (= 11) from $n = 27$ available tests] (Ap = anteroposterior direction, ML = mediolateral direction)

Components	Estimated error (E)	Measured RMS	Error as % of measured RMS
AP force (N)	0.72 (0.25)	2.42 (2.08)	62.7 (64.2)
ML force (N)	0.37 (0.18)	20.0 (4.04)	1.97 (1.12)
Vertical force (N)	1.29 (0.97)	375 (48.0)	0.34 (0.25)
Torque in sagittal plane (Nm)	0.86 (0.38)	10.5 (7.54)	15.7 (14.8)
Torque in coronal plane (Nm)	0.87 (0.49)	6.66 (5.89)	33.4 (43.8)

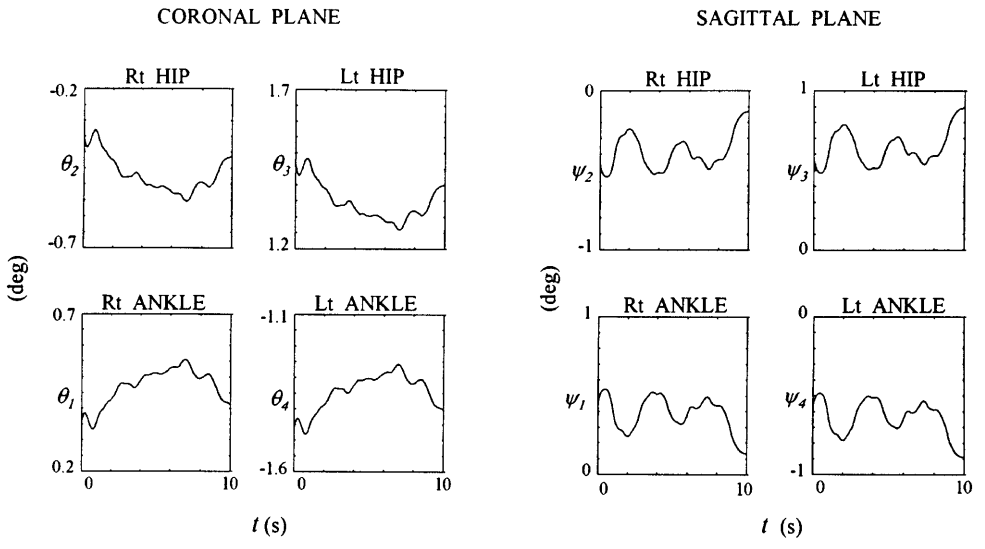

Fig. 5. Estimated kinematics of the segments in the coronal and sagittal planes ($\psi_i,\ i = 1, \ldots 4$) (Rt = right, Lt = left)

Table 2. Typical ranges of the predicted sagittal angular displacements of the ankle (our model) and of data available from the literature. Angular displacements were monitored by active markers (Fioretti et al. 1992b; Corradini et al. 1997) or linear potentiometers (Valk-Fai 1973). For the data presented by Fioretti et al. (1992b), only the mean (standard deviation) of the displacements were available

	Our model	Fioretti et al. (1992b)	Valk-Fai (1973)	Corradini et al. (1997)
Displacements (deg)	0.18–0.73	0.8 (0.2)	0.19–0.95	0.14–0.89

Curves of the acting torques in the joints are presented in Fig. 6 (subject El) for the coronal planes. Examination of the torque results of all the tests revealed the existence of a considerable mediolateral torque imbalance at the hip level. Least square linear regression was performed to examine the correlation between mediolateral torque imbalance and weight-bearing imbalance. The latter is defined as the difference between the average forces supported by the two legs and is expressed in percentage of body weight (Mizrahi and Susak 1989). The significance of variation coefficients was tested, using the F-test. Mediolateral torque imbalance was found to be in good correlation with weight-bearing imbalance, both in the ankle ($r = 0.89,\ P < 0.01$) and the hip level ($r = 0.96,\ P < 0.01$). No significant correlations were found between AP torque imbalance and weight-bearing imbalance ($r < 0.2,\ P > 0.05$).

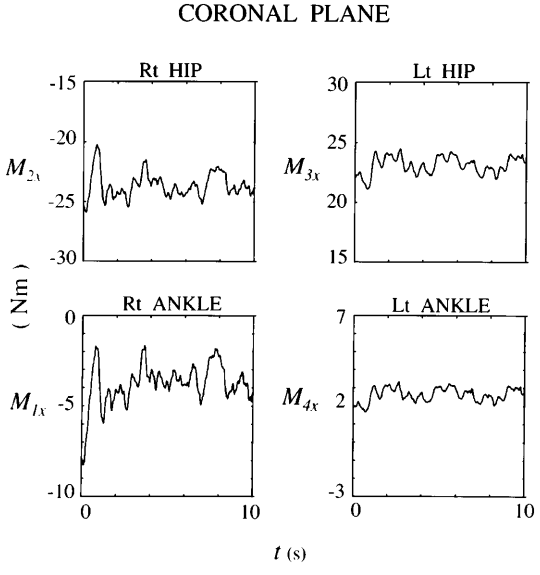

Fig. 6. Estimated dynamics (torques acting on each of the segments in the coronal plane ($\boldsymbol{M}_{ix},\ i = 1, \ldots 4$)

5 Discussion

The major objective of this study was to present a method for the estimation of the kinematics and the dynamics in the ankle and hip joints directly from bilateral measurements of force. A three-dimensional, four-joint, five-segment model of the human body compatible with a spatial four-bar mechanism was used. This model describes the motion of the CG of the body separately in the coronal and sagittal planes. Based on a previous study (Levin and Mizrahi 1996), the transverse components of the CG were obtained directly from the foot-ground reaction force data (2). These components, i.e., r_{GRx}, r_{GRy}, and r_{GRz}, served as inputs for the iterative algorithm (Fig. 2). The kinematics and the dynamics of the model (i.e., angular displacements of the segments and moments in the joints) were then resolved by forward kinematics and backward dynamics calculations (Fig. 2). It should be borne in mind that a thorough evaluation of the kinematics and dynamics of

the model is bounded by the uncertainty of the exact position of the joints and by the anthropometry of the subject (Riley et al. 1990). Consequently, the equation of motion was further constrained by including a condition which compared model results to actually measured data. Quantitative deviations between the model and measured dynamics (12) were evaluated and corrected iteratively (Fig. 2). In the first iteration, the initial positioning of the joints was set in accordance with the approximate position of the subject's feet on the platform frame and the anthropometric properties of each segment (evaluated by scaling data taken from the literature: Braune and Fischer 1987; Drillis and Contini 1966). In the subsequent iterations, these initial properties were readjusted to obtain a minimum of the mean square difference (12) between model and measured dynamics.

The results presented in Figs. 3 and 4 and in Table 1 indicate that by using the iterative algorithm, similarities between the model and measured dynamics of the right foot could be obtained. In the mediolateral and vertical forces, the model prediction was found to be accurate. Somewhat higher discrepancies between model and measured dynamics were found for the torque in the sagittal plane, and the relative error exceed 15% of the average RMS measured value. A relatively high dissimilarity between model and measured dynamics was observed for the anteroposterior force (Fig. 3) and for the torque in the coronal plane (Fig. 4). These differences between model and measured data, as shown in Table 1, reveal the following relative errors: 62.7% $\pm$ 64.2% for the anteroposterior force and 33.4% $\pm$ 43.8% for the mediolateral torque. The magnitude of the mean value of ε (14) obtained for the anteroposterior force was found to be of the same order of magnitude as the mean RMS value. It can thus be concluded that the model is limited by the ability to estimate the anteroposterior components of the force. On the other hand, our model demonstrated a high accuracy (relative error $<$ 2%) in estimating the mediolateral and vertical force components.

Similar methodologies were suggested by Vaughan et al. (1982b) in the application of an optimization approach to the closed loop problem in biomechanics. Prediction of the horizontal and vertical reaction forces at the distal segments was reasonably successful. In their study, Vaughan et al. (1982b) referred to the closed loop problem during walking up stairs, vertical jumping and cartwheeling, where the horizontal forces are expected to be significantly higher than those measured during postural sway activity. The optimization procedure used by Vaughan et al. (1982b) estimated the final trajectory of the point of application of the forces, acting on these segments. In our study, the estimated errors obtained for the torque and center of pressure in the final iteration were relatively high. This suggests that the evaluated positioning of the feet and the solved localization of the joints crucially affect the accuracy of the estimated kinematics and dynamics of the model. The failure of the iterative algorithm to establish an optimal solution (in 15 out of 44 tests) can be attributed to one or a combination of the following: (i) wrong positioning of the feet in the first iteration, since the boundaries of the location of the joints were calculated, assuming the location of the feet was similar for all tests and (ii) excessive sway, not allow the term $\dot{\mathbf{H}}$ in (1) to be ignored. Unfortunately, we did not have the ability to detect and hence correct the deviations of the actual initial location of the feet from their expected positioning, and therefore, to establish the exact cause of the non-convergence.

Table 2 discloses that there is a similarity in the range of angular displacements between our model and those reported in the reference studies, despite differences in methodologies and tested populations. For instance, in the compared studies, no bilateral results were reported because the right and the left lower limbs were combined together and treated as one support, resulting in essentially planar segmental models, as opposed to our three-dimensional, five-segment model. The similarity between our model and existing experimental results was not only in the range of angular displacements, but also in the range of CG motion. The fact that the relative motion between segments helps to diminish the horizontal excursion of the CG trajectory emerges from our results and was observed also by Valk-Fai (1973).

The angular displacements in the sagittal plane were found to be in phase or in opposite phase (Fig. 5). The patterns of the angular deviation on the right side (i.e., the right ankle and hip) in the model were found to be positive in sequence with the angular deviation on the left side (Fig. 5). Similar comparisons between the patterns of the angular displacements in the joints have been reported previously (Fioretti et al. 1992b; Kapteyn 1973). Additionally, the sagittal angular displacements in the joints of the hips were opposite in relation to the patterns of the ankle joints. These types of movements were observed previously by Valk-Fai (1973). It should be remembered that although direct measurements of the kinematics of the swaying body involve a considerable error, reaching the order of magnitude of the signal (Benda et al. 1994), the sequences of the patterns of the angular displacements are expected to be preserved.

Attention should be paid to the following observation: The patterns of the angular deviation in the ankles, both in the coronal and sagittal planes, were found to be in opposite phase to the angular deviation in the hips (Fig. 5). Conversely, the torques in the coronal and the sagittal planes at the ankle level were found to be in phase with the torques at the hip level (Fig. 6). It should be mentioned that the generalized coordinates (i.e., $\theta_1 \ldots \theta_4$ for coronal plane, and $\psi_1 \ldots \psi_4$ for the sagittal plane) were defined as the relative displacements between the lower and the upper segments, and the generalized torques (i.e., $M_{1x} \ldots M_{4x}$ for the coronal plane and $M_{1y} \ldots M_{4y}$ for the sagittal plane) were defined as the moment applied by the lower segment on the upper segment. Hence, when moving from ankle to hip, the relation between sequences of torque and angular displacement is inverted. Therefore, it can be concluded that, during postural sway, the mechanical power delivered to the segments by the muscles at the distal/proximal joint level is taken back by the muscles acting about the upper/lower joint. This may provide some

evidence for the central strategy of the body to keep the CG in a stable position and to minimize muscular activity while standing still. Such a strategy has been widely discussed in the literature (Andersson and Winters 1990; Keshner and Allum 1990; Penzer et al. 1995; Valk-Fai 1973).

The subjects in this study demonstrated a mediolateral torque imbalance between the right and left sides. The mediolateral torque imbalance and weight-bearing imbalance were found to be highly correlated, both in the ankle ($r = 0.89$, $P < 0.01$) and the hip ($r = 0.96$, $P < 0.01$). It has been previously reported that forces and positioning of the CG do not act symmetrically in subjects with pathologies (Isakov et al. 1992; Kapteyn 1973; Levin and Mizrahi 1996). Therefore, the mediolateral torque imbalance at the joints may indicate some minor orthopaedic disorders, such as the existence of a difference in length between the right and left sides. Voluntary activation of the lower extremities (e.g., slight flexion of the knee) is expected to demonstrate similar effects. It should be noted that the differences in length between the right and left sides can be modeled easily, by iterative updating of the lengths in order to reduce the mean square difference in (12). On the other hand, flexion of the knee adds an extra generalized coordinate to the model. Usage of the present model as a four-bar mechanism would, therefore, not be valid in this case.

Bilateral measurements of force and the model suggested in this study are suitable for the estimation of the dynamics of the subjects while standing still. The same methodology, however, could be expanded to estimate body kinematics and dynamics for any motion that is performed while keeping the foot flat on the platform, such as: (a) during the stance phase of gait, (b) standing on one foot, or (c) active swaying of the body. Moreover, estimation of the mechanical impedance in the joints of the lower extremity, power transfer through the joints, and the production of muscle forces are made possible if the torque and angles are known. It should be mentioned that the evaluation of the actual muscle forces would require incorporation of additional information aimed at reducing the model redundancy, including electromyographic measurements and/or optimization procedures derived from mechanical or energetic considerations.

Acknowledgements. This study was supported by the Segal Foundation and by the Fund for Promotion of Research at the Technion.

References

Andersson GBJ, Winters JM (1990) Role of muscle in postural tasks: spinal loading and postural stability. In: Winters JM, Woo SL-Y (eds) Multiple muscle systems: biomechanics and movement organization. Springer, Berlin Heidelberg New York, pp 149–164

Barin K (1989) Evaluation of generalized model of human postural dynamics and control in the sagittal plane. Biol Cybern 61:37–50

Benda BJ, Riley PO, Krebs DE (1994) Biomechanical relationship between center of gravity and center of pressure during standing. IEEE Trans Rehab Eng 2:3–10

Braune W, Fischer O (1987) The human gait. Springer, Berlin Heidelberg New York, pp 428–431

Corradini ML, Fioretti S, Leo T, Piperno R (1997) Early recognition of postural disorders in multiple sclerosis through movements analysis: a modeling study. IEEE Trans Biomed Eng 44:1029–1038

Drillis R, Contini R (1966) Body segment parameters. (Technical Report 1166.03) New York University, New York

Fioretti S, Leo T, Maurizi M, Fieroni G (1992a) A CAMA system for the functional evaluation of posture maintenance. Posture Gait Control Mech 2:67–70

Fioretti S, Leo T, Maurizi M, Franceschini M, Piperno R, Sttecchi S (1992b) Functional evaluation of multiple sclerotic patients at an early stage. Posture Gait Control Mech 2:63–66

Hunt KH (1978) Kinematics geometry of mechanisms. Oxford University Press, London, pp 31–37

Inman VT (1976) The joint of the ankle. W&W Company, Baltimore

Isakov E, Mizrahi J, Ring H, Susak Z, Hakim N (1992) Standing sway and weight bearing distribution in people with below-knee amputations. Arch Phys Med Rehabil 73:146–178

Isakov E, Mizrahi J, Susak Z, Onnu I, Hakim N (1994) Influence of prosthesis alignment on the standing balance of below-knee amputees. Clin Biomech 9:258–262

Kapteyn TS (1973) Afterthought about the physics and mechanics of the postural sway. Agressologie 14C:27–35

Keshner EA, Allum JH (1990) Muscle activation patterns coordinating postural stability from head to foot. In: Winters JM, Woo SL-Y (eds) Multiple muscle systems: biomechanics and movement organization. Springer, Berlin Heidelberg New York, 481–497

Levin O, Mizrahi J (1996) An iterative model for estimation of the trajectory of center of gravity from bilateral reactive force measurements in standing sway. Gait Posture 4:89–99

Mizrahi J, Susak Z (1989) Bilateral reactive force patterns in postural sway activity of normal subjects. Biol Cybern 6:279–305

Mizrahi J, Groswasser Z, Susak Z, Reider-Groswasser I (1989a) Standing posture of carniocerebral injured patients: bilateral reactive force patterns. Clin Phys Physiol Meas 10:25–37

Mizrahi J, Solzi P, Ring H, Nisell R (1989b) Postural stability in stroke patients: vectorial expression of asymmetry, sway-activity and relative sequence of reactive forces. Med Biol Eng Comput 27:181–190

Penzer VP, Bandinelli S, Hallett M (1995) Biomechanical assessment of quiet standing and changes associated with aging. Arch Phys Med Rehabil 76:151–157

Riley PO, Mann RW, Hodge AW (1990) Modelling of the biomechanics of posture and balance. J Biomech 23:503–506

Ring H, Mizrahi J (1991) Bilateral postural sway in stroke patients: new parameters for assessing and predicting locomotor outcome. J Neurol Rehabil 5:175–179

Ring H, Mizrahi J (1992) Biomechanical sway parameters in the evaluation of stroke patients. Neurorehabilitation 2:27–35

Saunders JB, Inman VT, Eberhart MB (1953) The major determinants in normal and pathological gait. J Bone Joint Surg [Am] 35:543–558

Snijders CJ, Verduin M (1973) Stabilograph, an accurate instrument for science interested in postural equilibrium. Agressologie 14C:15–20

Valk-Fai T (1973) Analysis of the dynamics behaviour of the body whilst standing still. Agressologie 14C:21–25

Vaughan CL, May JG, Andrews JG (1982a) Closed loop problems in biomechanics. Part I. A classification system. J Biomech 15:197–200

Vaughan CL, May JG, Andrews JG (1982b) Closed loop problems in biomechanics. Part II, An optimization approach. J Biomech 15:201–210